



Novel series of MLa_2WO_7 ($M = \text{Sr, Ba}$) microwave dielectric ceramic systems with monoclinic structures

Xianjie Zhou¹ · Huanfu Zhou¹ · Qiang Wu¹ · Xiaowen Luan¹ · Sang Hu¹ · Jiji Deng¹ · Shixuan Li¹ · Kuangguo Wang¹ · Xiuli Chen¹

Received: 26 December 2019 / Accepted: 19 May 2020
© Springer Science+Business Media, LLC, part of Springer Nature 2020

Abstract

Novel series of MLa_2WO_7 ($M = \text{Sr, Ba}$) ceramics were prepared via a traditional solid-state reaction method. The sintering characteristic, crystal structures, micromorphology and microwave dielectric performances of systems were systematically investigated. X-ray diffraction (XRD) and Rietveld refinement display that both $SrLa_2WO_7$ (SLW) and $BaLa_2WO_7$ (BLW) ceramics are monoclinic structure with Fdd (No. 14) space group. SLW and BLW ceramics have high relative density (more than 94%). The SLW ceramics sintered at 1400 °C exhibited good microwave dielectric performances with $\epsilon_r = 23.2$, $Q \times f = 29,720$ GHz, $\tau_f = -127$ ppm/°C and the BLW ceramics sintered at 1300 °C had excellent properties of $\epsilon_r = 25.3$, $Q \times f = 36,473$ GHz, $\tau_f = -108$ ppm/°C. These results show that MLa_2WO_7 ($M = \text{Sr, Ba}$) ceramics could be candidates for microwave devices.

1 Introduction

With the rapid development of mobile communication, the microwave dielectric materials should be miniaturization, low cost, high efficiency, nontoxicity, etc [1–5]. Moreover, the application of microwave materials should require three basic performances: an appropriate relative permittivity (ϵ_r) to satisfy the applications for different frequency ranges, a high quality factor ($Q \times f$) to decrease the power loss, and a near-zero temperature coefficient of resonant frequency (τ_f) to ensure the temperature stability of devices [6–10]. Currently, the application of microwave dielectric materials is becoming more and more extensive in military and commercial terms; the materials have been commonly applied in communication systems, especially for the fifth generation (5G) telecommunication which the characteristics are fast transmission speed [11, 12]. Therefore, to better adapt to the

5G new era technology tide, researchers need to study the improvement of material properties such as using different preparation methods (sol–gel method, hot-press sintering method, plasma sputtering method), adding vary sintering aids (B_2O_3 , MnO_2 , V_2O_5) and discover new materials to replace the original materials to meet the needs of products.

Researchers have been paying attention to the titanium-based, molybdenum-based, vanadium-based, silicon-based, germanium-based and tungsten-based ceramics for better microwave dielectric properties. Especially, the tungsten-based ceramics exhibited good microwave dielectric properties because the W^{6+} has good ionic polarization of [W–O] polyhedron. For example, Sebastian et al. [13] reported that the $Sr_2La_2MgW_2O_{12}$ ceramics sintered at 1525 °C had microwave dielectric performances of $\epsilon_r = 24.7$, $Q \times f = 35,000$ GHz, and $\tau_f = -83$ ppm/°C, but high sintering temperature limited its further commercial applications. $La_6Mg_4A_2W_2O_{24}$ ($A = \text{Ta and Nb}$) ceramics possessed microwave dielectric properties of $\epsilon_r = 25.2$, $Q \times f = 13,600$ GHz, and $\tau_f = -45$ ppm/°C for $La_6Mg_4Ta_2W_2O_{24}$ ceramic sintered at 1350 °C, and $\epsilon_r = 25.8$, $Q \times f = 16,400$ GHz, and $\tau_f = -56$ ppm/°C for $La_6Mg_4Nb_2W_2O_{24}$ ceramics sintered at 1400 °C; however, the expensive of the raw materials (Nb_2O_5 and Ta_2O_5) hindered their further applications [14]. Therefore, to find a better tungsten-based microwave dielectric performance material, MLa_2WO_7 ($M = \text{Sr, Ba}$) ceramics were designed. Furthermore, the sintering characteristic,

✉ Huanfu Zhou
zhouhuanfu@163.com

¹ Guangxi Ministry-Province Jointly-Constructed Cultivation Base for State Key Laboratory of Processing for Non-Ferrous Metal and Featured Materials, Guangxi Key Laboratory in Collaborative Innovation Center for Exploration of Hidden Nonferrous Metal Deposits and Development of New Materials in Guangxi, School of Materials Science and Engineering, Guilin University of Technology, Guilin 541004, China

phase structure, microstructure and microwave dielectric performances of ceramics were also investigated.

2 Experimental procedure

The MLa_2WO_7 ($M = \text{Sr}, \text{Ba}$) ceramics were prepared via the traditional solid-state reaction method using SrCO_3 ($\geq 99\%$), BaCO_3 ($\geq 99\%$), La_2O_3 ($\geq 99\%$), and WO_3 ($\geq 99\%$) as the raw materials. The rare-earth oxide of La_2O_3 was hygroscopic, so La_2O_3 was preheated at 900°C for 2 h to remove the moisture before weighing. The raw powders were weighted according to the stoichiometric of MLa_2WO_7 ($M = \text{Sr}, \text{Ba}$) and ball-milled in the ethanol media for 6 h with ZrO_2 balls. After drying, the mixtures were calcined at 1150°C for 4 h, and the calcined powders were milled with ZrO_2 balls for 6 h in ethanol again. After drying and sieving, the powders were added 7wt% polyvinyl alcohol solution and pressed into pellets with ~ 12 mm in diameter and ~ 6.0 mm in height under a pressure of 150 MPa. Finally, the pellets were sintered at 1250 – 1450°C for 4 h.

The phase purity of product ceramic powders was analyzed by an X-ray diffraction (XRD; Model X Pert PRO, Almelo, the Netherlands). The microstructure on surface of the samples was observed by a scanning electron microscopy (JSM6380-LVSEM, Japan). Microwave dielectric performances of specimens were measured by a network analyzer (Model E5071 CENA, USA) at a room temperature environment. The temperature coefficient of resonant frequency was calculated by $\tau_f = \Delta f / (f_0 \Delta T)$ in the temperature range from 25 to 85°C .

3 Results and discussion

Figure 1 shows the XRD patterns of MLa_2WO_7 ($M = \text{Sr}, \text{Ba}$) ceramics sintered at different temperatures. The diffraction peaks of all samples are matched well with the JCPDS

01-077-2426, 049-0353, respectively, indicating that the MLa_2WO_7 (Sr, Ba) ceramics belong to a monoclinic structure with Fdd (No. 14) space group. With rising the sintering temperature, BLW ceramics exhibited a single pure phase, but SLW ceramics had a second phase peak. With increasing the sintering temperature, diffraction peak position of samples kept stable, showing that the cell volume of ceramics did not changed. In addition, to further explore the cations occupancy in ceramics, the Rietveld refinement in view of XRD profile for BLW ceramics sintered at $1300^\circ\text{C}/4$ h was done and the result is demonstrated in Fig. 2. The Bragg strength was very close to experimental data and gained as $R_p = 7.07\%$, $R_{wp} = 10.36\%$, and $\chi^2 = 5.21$, which indicated that the data are credible. Meanwhile, the refinement parameters are listed in the Table 1. It can be seen that $[\text{WO}_6]$ octahedron, $[\text{BaO}_6]$ octahedron and $[\text{LaO}_8]$ dodecahedron share an oxygen atom, and $[\text{WO}_6]$ octahedron was used as an intermediate bridge to form the structural framework of BLW ceramics.

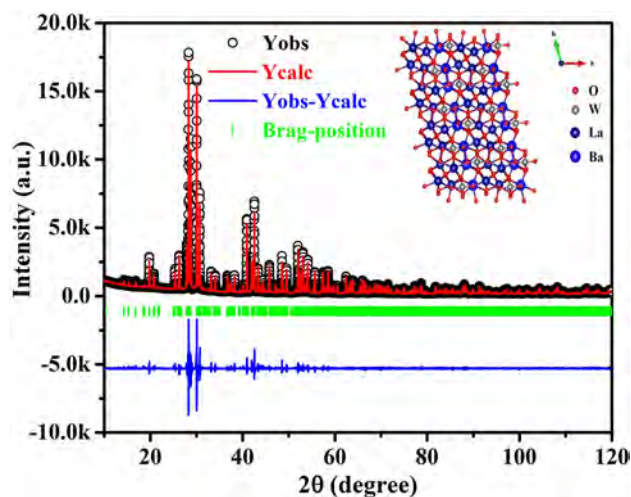


Fig. 2 Rietveld refinement and crystal structure of BLW ceramics sintered at 1300°C

Fig. 1 XRD patterns of MLa_2WO_7 ceramics: (a) $M = \text{Sr}$, (b) $M = \text{Ba}$

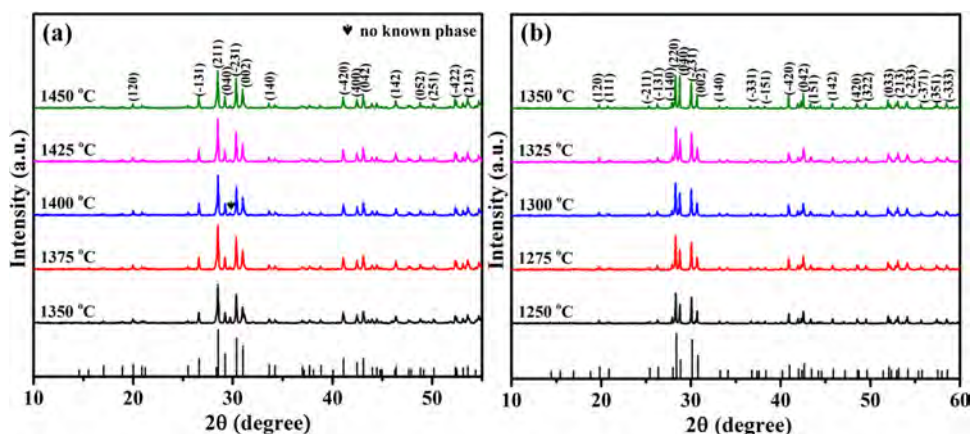


Table 1 Refinement parameters of BLW ceramics sintered at 1300 °C

BaLa ₂ WO ₇	Lattice parameters (Å)			Lattice parameters (Å)			Vol (Å ³)
	<i>a</i>	<i>b</i>	<i>c</i>	<i>α</i>	<i>β</i>	<i>γ</i>	
	8.8579	12.8725	5.8303	90.0000	90.0000	105.1233	641.773
	<i>x</i>		<i>y</i>	<i>z</i>		Occupancy	
W1	0.4791		0.5071	0.2226		0.9818	
W2	0.9130		0.8277	0.2752		1.0141	
Ba1	0.6764		0.2997	0.2370		1.0444	
Ba2	0.7141		0.0318	0.2719		0.9920	
La1	0.0018		0.5824	0.2421		0.9770	
La2	0.3945		0.7505	0.2640		1.0033	
La3	0.1322		0.3006	0.2658		0.9865	
La4	0.2639		0.0345	0.2340		1.0031	
O1	0.6471		0.8067	0.2013		1.2082	
O2	0.4459		0.5423	− 0.0301		0.8738	
O3	0.9416		0.2384	0.4602		1.0298	
O4	0.4663		0.5705	0.5065		1.2791	
O5	0.1492		0.8272	0.2225		1.0540	
O6	0.2622		0.5014	0.1642		1.0838	
O7	0.7053		0.5328	0.1805		1.1497	
O8	0.9250		0.7320	0.0160		1.2960	
O9	0.4660		0.9230	0.0520		1.2370	
O10	0.4420		0.3830	0.4120		1.1904	
O11	0.9900		0.5068	0.9026		1.2247	
O12	0.9390		0.4399	0.5474		0.8778	
O13	0.2016		0.6422	0.4953		1.0550	
O14	0.2016		0.1924	− 0.0012		1.1031	

Figure 3 illustrates the SEM photographs of MLa_2WO_7 ($M = \text{Sr, Ba}$) ceramics sintered at different temperatures. The grains were tightly connected and had a clear grain boundary, no liquid phase appeared in all samples. As the sintering temperature increases, the grain size of ceramics gradually increases and further tends to inhomogeneous. In particular, too high sintering temperature will result in the pores between the grains or the crack, as shown in Fig. 3c, f. The EDS analysis consequence reveals that all elements ratios are approximate to the chemical composition of the MLa_2WO_7 ($M = \text{Sr, Ba}$) ceramics, as listed in Table. 2.

Figure 4 shows the bulk density and relative density as a function of the sintering temperature for MLa_2WO_7 ($M = \text{Sr, Ba}$) ceramics. The theoretical densities of SLW ceramics and BLW ceramics were obtained by the XRD analysis software and the values are 7.05 g/cm³ and 7.36 g/cm³, respectively. All samples have high density (more than 94% of relative density). The densities of SLW ceramics and BLW ceramics were increased firstly and then decreased with the change of sintering temperature. The highest density of SLW ceramics and BLW ceramics were 6.87 g/cm³ and 7.21 g/cm³ as the

sintering temperatures were 1300 °C and 1400 °C, respectively. However, the densities of the MLa_2WO_7 ($M = \text{Sr, Ba}$) ceramics were reduced continuously with increasing the sintering temperature, which could be the over-sintering, as shown in Fig. 3c, f.

It was well known that the relative permittivity is affected by the internal factors (crystal structure, packing fraction, lattice energy, material composition) and the external factors (defects such as grain boundaries, pores, liquid phase) [15–19]. Initially, the relative permittivity of ceramics increased significantly with increasing the sintering temperature, and decreased with further increasing the sintering temperature, as shown in Fig. 4. Obviously, the changing trend of MLa_2WO_7 ($M = \text{Sr, Ba}$) ceramics in ϵ_r was in accordance with the density. To minimize the effect of the pore on ϵ_r , the corrected relative permittivity (ϵ_{corr}) was obtained by the Bosman and Having's formula [20]:

$$\epsilon_{\text{corr}} = \epsilon_r(1 + 1.5p) \quad (1)$$

where P is the fraction porosity, ϵ_{corr} and ϵ_r are the corrected and measured values of the permittivity, respectively.

Fig. 3 SEM images of $M\text{La}_2\text{WO}_7$ ($M=\text{Sr}, \text{Ba}$) ceramics sintered at **a** 1275 °C, **b** 1300 °C, **c** 1325 °C for SLW ceramics, **d** 1375 °C, **e** 1400 °C, **f** 1425 °C for BLW ceramics

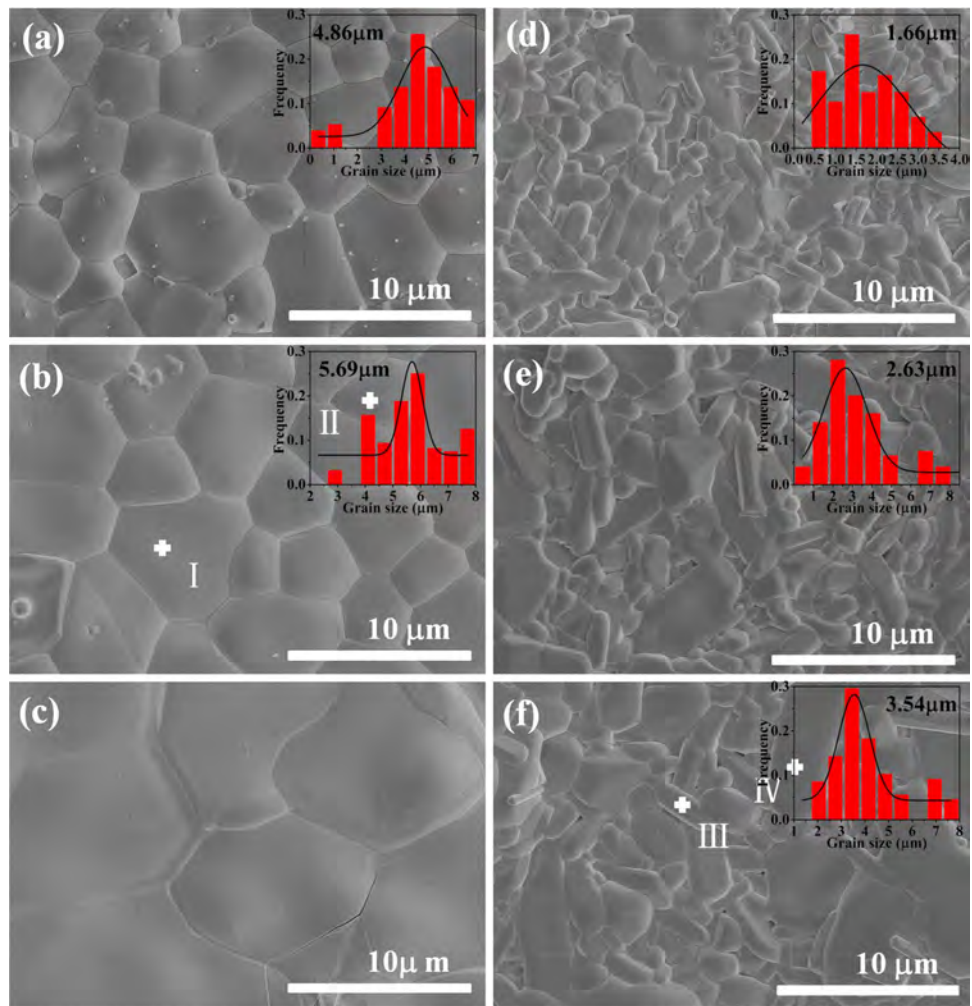


Table 2 EDS results of $M\text{La}_2\text{WO}_7$ ($M=\text{Sr}, \text{Ba}$) ceramics

Spot	Element (%)				
	Sr	Ba	La	W	O
I	14.15		20.78	9.96	55.11
II	13.03		17.84	8.93	60.20
III		9.68	18.85	10.72	60.72
IV		9.01	17.11	10.06	63.81

The corrected value ($\mathcal{E}_{\text{corr}}$) was always higher than that of the measured value (\mathcal{E}_r), as shown in Fig. 4.

The quality factor and temperature coefficient of resonant frequency for $M\text{La}_2\text{WO}_7$ ($M=\text{Sr}, \text{Ba}$) ceramics are shown in Fig. 5. Initially, it can be discovered that the quality factor of ceramics was increased to a maximum of 29,720 GHz for SLW ceramics, and 36,473 GHz for BLW ceramics, respectively, which was the similar with the density, demonstrating that the density was a key indicator in microwave dielectric performance. The quality factor value of SLW and BLW ceramics decreased as

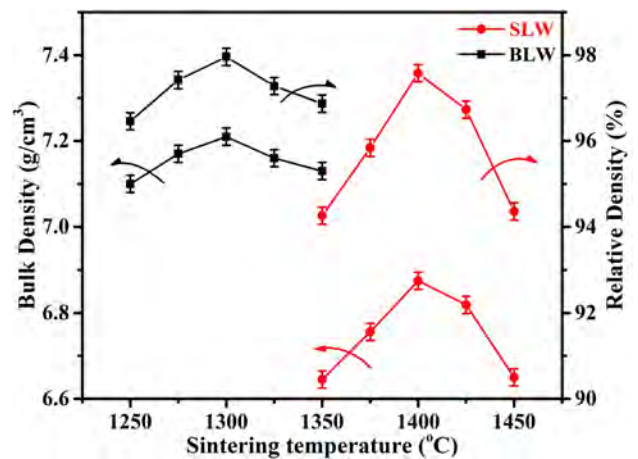


Fig. 4 Bulk density and relative density of $M\text{La}_2\text{WO}_7$ ($M=\text{Sr}, \text{Ba}$) ceramics as a function of sintering temperatures

the sintering temperature exceeds 1300 °C and 1400 °C, respectively, which may be due to the abnormal grain growth or grain cracks, as shown in Fig. 3c. The τ_f

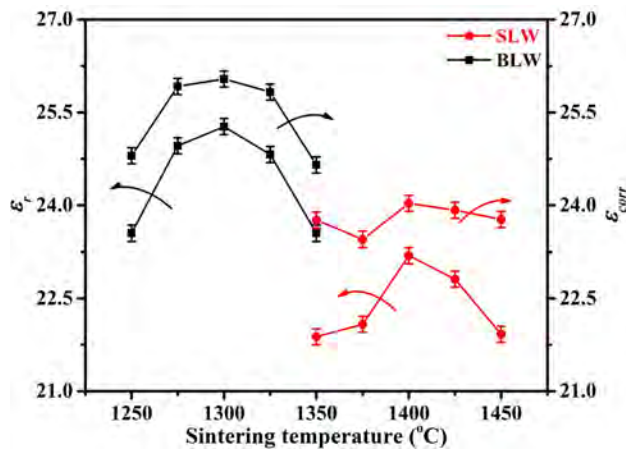


Fig. 5 ϵ_r and ϵ_{corr} of MLa_2WO_7 ($M = \text{Sr, Ba}$) ceramics as a function of sintering temperatures

of MLa_2WO_7 ($M = \text{Sr, Ba}$) ceramics has a large negative value. The MLa_2WO_7 ($M = \text{Sr, Ba}$) ceramics could adjust the τ_f value to near zero by adding an appropriate amount of CaTiO_3 . Table 3 lists the comparison of the microwave dielectric properties for some compounds with similar relative permittivity. The SrNdGaO_4 [21], $\text{Ba}_5\text{Nb}_3\text{TaO}_{15}$ [24] and $\text{Ca}(\text{Gd}_{1/2}\text{Ta}_{1/2})\text{O}_3$ [26] ceramics have the near-zero τ_f values, but high raw materials of GaO_2 and Ta_2O_5 restricted their further applications. LaYbO_3 [25], SmZrTaO_6 [22] and BaHfO_3 [23] ceramics exhibited poor dielectric performance and high sintering temperatures. Although SrLaGaO_4 [21] has a low sintering temperature, the quality value is inferior. By contrast, the MLa_2WO_7 ($M = \text{Sr, Ba}$) ceramics have cheaper raw materials and low sintering temperature, indicating that these materials could be the candidates for microwave devices (Fig. 6).

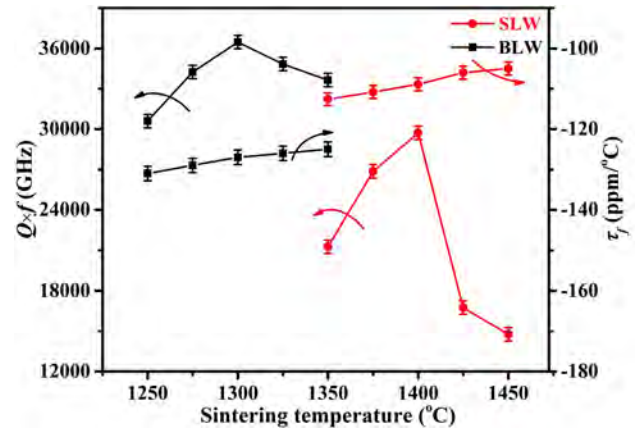


Fig. 6 $Q \times f$ and τ_f value of MLa_2WO_7 ($M = \text{Sr, Ba}$) ceramics as a function of sintering temperatures

4 Conclusions

In this work, MLa_2WO_7 ($M = \text{Sr, Ba}$) ceramics have been prepared via the traditional solid-state reaction method. The MLa_2WO_7 ($M = \text{Sr, Ba}$) ceramics belong to the monoclinic structure. The density of samples had a close relationship with the relative permittivity and quality factor value. The SLW ceramics exhibited good microwave dielectric performances with $\epsilon_r = 23.2$, $Q \times f = 29,720$ GHz, $\tau_f = -127$ ppm/°C. The BLW ceramics had excellent microwave dielectric properties with $\epsilon_r = 25.3$, $Q \times f = 36,473$ GHz, $\tau_f = -108$ ppm/°C. In next work, an appropriate amount of CaTiO_3 was added to adjust the temperature coefficient of resonance frequency of MLa_2WO_7 ($M = \text{Sr, Ba}$) ceramics to near zero.

Table 3 Comparison of the microwave dielectric properties for some compounds with similar relative permittivity

Material systems	Sintering temperature (°C)	ϵ_r	$Q \times f$ (GHz)	τ_f (ppm/°C)	Refs.
SrLaGaO_4	1275	20.3	16,200	-34	[21]
SmZrTaO_6	1650	21.2	24,190	-58	[22]
SrNdGaO_4	1300	21.4	16,600	7	[21]
BaHfO_3	1750	24.2	14,250	111	[23]
$\text{Ba}_5\text{Nb}_3\text{TaO}_{15}$	1500	25.7	21,600	16	[24]
LaYbO_3	1600	26.0	20,600	-22	[25]
$\text{Ca}(\text{Gd}_{1/2}\text{Ta}_{1/2})\text{O}_3$	1600	27.2	26,000	-16	[26]
SrLa_2WO_7	1400	23.3	29,720	-127	This work
BaLa_2WO_7	1300	25.3	36,473	-108	This work

Acknowledgements This work was supported by the Natural Science Foundation of China (Nos. 61761015 and 11664008), Natural Science Foundation of Guangxi (Nos. 2017GXNSFFA198011 and 2017GXNSFDA198027).

References

1. D. Zhou, L.X. Pang, D.W. Wang, Z.M. Qi, I.M. Reaney, High quality factor, ultralow sintering temperature $\text{Li}_6\text{B}_4\text{O}_9$ microwave dielectric ceramics with ultralow density for antenna substrates. *ACS. Sustain. Chem. Eng.* **6**, 11138–11143 (2018)
2. B. Tang, Q. Xiang, Z. Fang, X. Zhang, Z. Xiong, H. Li, C. Yuan, S. Zhang, Influence of Cr^{3+} substitution for Mg^{2+} on the crystal structure and microwave dielectric properties of $\text{CaMg}_{1-x}\text{Cr}_{2x/3}\text{Si}_2\text{O}_6$ ceramics. *Ceram. Int.* **45**, 11484–11490 (2019)
3. A. Feteira, D.C. Sinclair, Microwave dielectric properties of low firing temperature $\text{Bi}_2\text{W}_2\text{O}_9$ ceramics. *J. Am. Ceram. Soc.* **91**, 1338–1341 (2008)
4. H.F. Zhou, N. Wang, J.Z. Gong, G. Fan, X.L. Chen, Processing of low-fired glass-free $\text{Li}_2\text{MgTi}_3\text{O}_8$ microwave dielectric ceramics. *J. Alloy. Compd.* **688**, 8–13 (2016)
5. S. Zhai, P. Liu, D. Liu, Y. Chu, Z. Yang, Low-firing $\text{Li}_4\text{Mg}_3\text{Ti}_2\text{O}_9$ – CaTiO_3 composite ceramics with temperature stable microwave dielectric properties. *J. Mater. Sci. Mater. Electron.* **30**, 20002–20009 (2019)
6. W. Lei, Z.Y. Zou, Z.H. Chen, B. Ullah, A. Zeb, X.K. Lan, W.Z. Lu, G.F. Fan, X.H. Wang, X.C. Wang, Controllable τ_f value of barium silicate microwave dielectric ceramics with different Ba/Si ratios. *J. Am. Ceram. Soc.* **101**, 25–30 (2018)
7. H. Zhou, X. Tan, J. Huang, N. Wang, G. Fan, X. Chen, Phase structure, sintering behavior and adjustable microwave dielectric properties of $\text{Mg}_{1-x}\text{Li}_x\text{Ti}_x\text{O}_{1+2x}$ solid solution ceramics. *J. Alloy. Compd.* **696**, 1255–1259 (2017)
8. K. Du, X.Q. Song, J. Li, W.Z. Lu, X.C. Wang, X.H. Wang, W. Lei, Phase compositions and microwave dielectric properties of Sn-deficient Ca_2SnO_4 ceramics. *J. Alloy. Compd.* **802**, 488–492 (2019)
9. G.H. Chen, J.S. Chen, X.L. Kang, Y. Luo, Q. Feng, C.L. Yuan, Y. Yang, T. Yang, Structural and microwave dielectric properties of new $\text{CaTi}_{1-x}(\text{Al}_{0.5}\text{Nb}_{0.5})_x\text{O}_3$ thermally stable ceramics. *J. Alloy. Compd.* **675**, 301–305 (2016)
10. J.S. Chen, G.H. Chen, X.L. Kang, Y. Luo, Y. Yang, T. Yang, C.L. Yuan, C.R. Zhou, Microstructure and microwave dielectric properties of $\text{BaNd}_2\text{Ti}_{4-x}\text{Al}_{4x/3}\text{O}_{12}$ ceramics. *J. Mater. Sci. Mater. Electron.* **27**, 8234–8241 (2016)
11. K. Wang, H. Zhou, X. Liu, W. Sun, X. Chen, H. Ruan, A lithium aluminium borate composite microwave dielectric ceramic with low permittivity, near-zero shrinkage, and low sintering temperature. *J. Eur. Ceram. Soc.* **39**, 1122–1126 (2019)
12. S. Liu, B. Tang, M. Zhou, P. Zhao, Q. Xiang, X. Zhang, Z. Fang, S. Zhang, Microwave dielectric characteristics of high permittivity $\text{Ca}_{0.35}\text{Li}_{0.25}\text{Nd}_{0.35}\text{Ti}_{1-x}(\text{Zn}_{1/3}\text{Ta}_{2/3})_x\text{O}_3$ ceramics ($x = 0.00$ – 0.12). *Ceram. Int.* **45**, 8600–8606 (2019)
13. V. Venugopal, P.S. Anjana, O. Parkash, D. Kumar, M.T. Sebastian, Synthesis, characterization, and microwave dielectric properties of $\text{Sr}_{2-x}\text{La}_2\text{Mg}_{1+x}\text{W}_3\text{O}_{12}$ ($x=0, 1$) ceramics. *J. Am. Ceram. Soc.* **93**, 2467–2469 (2010)
14. R. Rajamma, M.T. Sebastian, Microwave dielectric properties of $\text{La}_6\text{Mg}_4\text{A}_2\text{W}_2\text{O}_{24}$ [$A=\text{Ta}$ and Nb] ceramics. *J. Am. Ceram. Soc.* **90**, 2472–2475 (2007)
15. H.L. Pan, Y.X. Mao, L. Cheng, H.T. Wu, New $\text{Li}_3\text{Ni}_2\text{NbO}_6$ microwave dielectric ceramics with the orthorhombic structure for LTCC applications. *J. Alloy. Compd.* **723**, 667–674 (2017)
16. M. Xiao, Y. Wei, Q. Gu, Z. Zhou, P. Zhang, Relationships between bond ionicity, lattice energy, bond energy and the microwave dielectric properties of $\text{La}(\text{Nb}_{1-x}\text{Ta}_x)\text{O}_4$ ($x = 0$ – 0.10) ceramics. *J. Alloy. Compd.* **775**, 168–174 (2019)
17. W.B. Li, D. Zhou, D. Guo, L.X. Pang, G.H. Chen, Z.M. Qi, Q.P. Wang, H.C. Liu, Structure, Raman spectra, far-infrared spectra and microwave dielectric properties of temperature independent $\text{CeVO}_4\text{TiO}_2$ composite ceramics. *J. Alloy. Compd.* **694**, 40–45 (2017)
18. H. Zhou, X. Tan, X. Chen, H. Ruan, Effect of raw materials pre-treated by physical grinding method on the sintering ability and microwave dielectric properties of $\text{Li}_2\text{MgTiO}_4$ ceramics. *J. Alloy. Compd.* **731**, 839–843 (2018)
19. H. Zhou, J. Gong, N. Wang, X. Chen, A novel temperature stable microwave dielectric ceramic with low sintering temperature and high quality factor. *Ceram. Int.* **42**, 8822–8825 (2016)
20. W. Liu, R. Zuo, A novel low-temperature fireable $\text{La}_2\text{Zr}_3(\text{MoO}_4)_9$ microwave dielectric ceramic. *J. Eur. Ceram. Soc.* **38**, 339–342 (2018)
21. X.Q. Liu, X.M. Chen, Microwave dielectric characteristics of SrLaGaO_4 and SrNdGaO_4 ceramics. *J. Eur. Ceram. Soc.* **26**, 1969–1971 (2006)
22. T. Oishi, A. Kan, H. Ohsato, H. Ogawa, Crystal structure–microwave dielectric property relations in $\text{Sm}(\text{Nb}_{1-x}\text{Ta}_x)(\text{Ti}_{1-y}\text{Zr}_y)\text{O}_6$ ceramics. *J. Eur. Ceram. Soc.* **26**, 2075–2079 (2006)
23. A. Feteira, D.C. Sinclair, K.Z. Rajab, M.T. Lanagan, Crystal structure and microwave dielectric properties of alkaline-earth hafnates, AHfO_3 ($A=\text{Ba}, \text{Sr}, \text{Ca}$). *J. Am. Ceram. Soc.* **91**, 893–901 (2008)
24. I.N. Jawahar, M.T. Sebastian, P. Mohanan, Microwave dielectric properties of $\text{Ba}_{5-x}\text{Sr}_x\text{Ta}_4\text{O}_{15}$, $\text{Ba}_5\text{Nb}_x\text{Ta}_{4-x}\text{O}_{15}$ and $\text{Sr}_5\text{Nb}_x\text{Ta}_{4-x}\text{O}_{15}$ ceramics. *Mater. Sci. Eng. B.* **106**, 207–212 (2004)
25. A. Feteira, L.J. Gillie, R. Elsebrock, D.C. Sinclair, Crystal structure and dielectric properties of LaYbO_3 . *J. Am. Ceram. Soc.* **90**, 1475–1482 (2008)
26. M.T. Sebastian, L.A. Khalam, S. Thomas, Temperature-stable and low-loss dielectrics in the $\text{Ca}(\text{B}'_{1/2}\text{Ta}_{1/2})\text{O}_3$ [$\text{B}'=\text{Lanthanides}, \text{Y}, \text{and In}$] system. *J. Am. Ceram. Soc.* **90**, 2476–2483 (2007)

Publisher's Note Springer Nature remains neutral with regard to jurisdictional claims in published maps and institutional affiliations.